

## **Winter-time variability of the Eastern Arabian Sea – A comparison between 2003 and 2013**

**Jayu Narvekar, Joshua Rosario D'Mello, S. Prasanna Kumar\*, Priyanka Banerjee<sup>1</sup>, Vrinda Sharma and Prachi Shenai-Tirodkar**

CSIR-National Institute of Oceanography, Dona Paula, Goa-403 004, India.

<sup>1</sup>Centre for Atmospheric and Oceanic Sciences, Indian Institute of Science, Bangalore, India

\* Corresponding author

Email: [prasanna@nio.org](mailto:prasanna@nio.org)

Telephone: +91-832-2450300

Fax: +91-832-2450608

**Running Title:** Eastern Arabian Sea winter-time variability

### **Abstract**

The Eastern Arabian Sea (EAS) is a region of complex interplay between several spatially and temporally varying oceanographic processes. Using two sets of in-situ data collected from the same stations, separated by a decade, we show that warming and cooling in the EAS was linked to the long-term variability of this region. Though the warming in the southern part of EAS was consistent with the basin-wide rise in SST in the Arabian Sea (AS), the enhanced freshening was a remote response to episodic events mediated by the strengthening of inter-basin exchange between Bay of Bengal (BoB) and AS through East India Coastal Current (EICC) and West India Coastal Current (WICC). The increased stratification in the southern part of EAS led to the decline in the chlorophyll over the decade. In contrast, enhanced chlorophyll in the northern part of the EAS over the decade was linked to the increased wind speed.

## 1. Introduction

The Eastern Arabian Sea (EAS), being a part of the tropical basin in the northern Indian Ocean, experiences strong seasonality forced by semi-annually reversing monsoon winds. Accordingly, the surface circulation along the EAS (western shelf of India) also reverses semi-annually. The West India Coastal current (WICC) flows pole-ward during winter monsoon (November to February) and equator-ward during summer monsoon (June to September) [Shetye *et al.*, 1991]. In summer, WICC carries high salinity waters from northern Arabian Sea (AS) towards south along the shelf-slope regions, while low salinity waters from the Bay of Bengal (BoB) is carried northward during winter [Prasanna Kumar *et al.*, 2004 and references therein]. Several distinct processes occurring in the EAS have the potential to impact the basin-scale oceanography. For example, the coastal upwelling occurring along the south EAS during summer monsoon [Wyrki, 1971] enhances primary productivity well beyond the shelf-slope regions off peninsular India and Sri Lanka [Smitha *et al.*, 2008]. Associated with this, the occurrence of a seasonal hypoxia is another characteristic feature of this region [Naqvi *et al.*, 2000], which has implications for ecosystems and fisheries. During winter south EAS is characterized by the occurrence of thermal inversions [Thadathil and Gosh, 1992; Durand *et al.*, 2004; Kurian and Vinayachandran, 2006], while northern part of the EAS comes under the influence of winter convection leading to winter blooms [Madhupratap *et al.*, 1996; Prasanna Kumar and Prasad, 1996]. In spring-summer transition (April-May), a mini-warm pool develops in south EAS, which augments the formation of monsoon onset vortex [Joseph, 1990; Rao and Sivakumar, 1999; Harish Kumar *et al.*, 2009; Nyadjro *et al.*, 2012]. The mini-warm pool has been shown to impact the onset of monsoon and the rainfall over India [Sanil Kumar *et al.*, 2004]. Though the occurrence of mini-warm pool is a regular feature of the seasonal cycle of SST in the SEA, no such regularity is seen in the occurrence of monsoon onset vortex [Vinachandran *et al.*, 2007].

Several studies have addressed the seasonal processes occurring in this region based on the analysis of individual cruise data and/or model simulations. However, studies on the inter-annual or decadal-scale variability are sparse. Recent, studies based on the sea surface temperature (SST) since 1950 have indicated that the western tropical Indian Ocean is warming up faster than the rest of the tropical regions of the world ocean [Roxy *et al.*, 2014]. In the AS the basin-averaged rate of warming since 1960 is between 0.10 to 0.12°C/decade [Prasanna Kumar *et al.*, 2009; Dinesh Kumar *et al.*, 2016]. However, it is not clear whether warming of the upper ocean has its impact in the subsurface layers in the EAS which houses several distinct oceanic processes (see Figure 1). It is in this context

that the present study attempts to unravel the water-column variability in the EAS during two winters separated by a decade, based on in-situ data. Further, we examine whether the observed difference is a part of the long-term change that the AS is experiencing.

## 2. Data and Methodology

Multi-disciplinary in-situ data collected from the same stations along the EAS from 8 to 21°N (Figure 1) during 2003 and 2013 following the JGOFS protocol [UNESCO, 1994] were used in the study. During 2003 the data were collected on board FORV *Sagar Sampada* from 13<sup>th</sup> January to 8<sup>th</sup> February (designated as winter 2002), while during 2013 it was onboard RV *Sindhu Sankalp* from 15<sup>th</sup> January to 3<sup>rd</sup> February 2013 (designated as winter 2012). The Conductivity- Temperature- Depth (CTD) profiles from surface to very close to the bottom were taken at 1-degree interval using Sea-Bird Electronics CTD. Water samples were collected from discrete depths (surface, 10m, 20m, 30m, 50m, 80m) using 1.7L/5L Niskin bottles fitted to the CTD rosette. These samples were used for determining chlorophyll *a* using Turner fluorometer. In addition, satellite derived monthly mean chlorophyll *a* data were extracted from MODIS aqua having 4km resolution for the period 2002 to 2014 ([http://oceandata.sci.gsfc.nasa.gov/MODIS-Aqua/Mapped/Monthly/4km/chlor\\_a/](http://oceandata.sci.gsfc.nasa.gov/MODIS-Aqua/Mapped/Monthly/4km/chlor_a/)). Note that for the above data NASA reprocessing R2014.0 was used. The data on v-component of geostrophic current were derived from AVISO merged product (<http://www.aviso.altimetry.fr/en/data.html>) for the month of January for the year 2001 to 2016. The data were extracted for a 1-degree longitude-by-1-degree latitude grid in such a way that the station indicated in the location map is at its centre. The monthly mean SST data and u-wind and v-wind data for the period 1960 to 2015 were obtained from the International Comprehensive Ocean-Atmosphere Data Set (ICODS) ([www.esrl.noaa.gov/psd/data/gridded/data.coads.1deg.html](http://www.esrl.noaa.gov/psd/data/gridded/data.coads.1deg.html)), which contains global monthly mean values on a 1-degree longitude by 1-degree latitude spatial grid [Woodruff *et al.*, 2011]. A 60-month running average was applied to the monthly mean SST data in order to remove the inter-annual variability. From the u and v winds the wind speed was calculated. The surface salinity data from 2001 to 2016 was from the gridded Argo monthly data on 1-degree longitude by 1-degree latitude grid ([www.jamstec.go.jp/ARGO/argo\\_web](http://www.jamstec.go.jp/ARGO/argo_web)). The temperature and salinity data obtained from the CTD was further used for the computation of static stability parameter following Pond and Pickard [1983].

$$E = -1/\rho [\partial\rho/\partial z]$$

Where E is the static stability parameter ( $\text{m}^{-1}$ ),  $\rho$  is the density ( $\text{kg m}^{-3}$ ) of the water and z is the depth (m).

### 3. Results and discussion

We first examined the spatial distribution of surface as well as water column temperature, salinity and chlorophyll *a* to decipher the latitudinal pattern present in the data during 2003 and 2013. Subsequently, the temporal variability of the surface parameters was explored in the context of long-term changes from this region, to ascertain if the observed variability is a part of the long-term variability.

#### 3.1 Spatio-temporal variability

The SST along the EAS showed similar north-south variability during 2003 and 2013, with values north of 17°N showing a rapid decrease with latitude (Figure 2a). The SST in the region south of 17°N varied between 27.8 and 28.8°C for both the years. However, in the region north of 17°N, the SST decreased from 28.3 to 25.3°C in 2003 and from 27.8 to 24.8°C in 2013. Though the spatial variability had similar pattern, SST in 2003 was warmer than that of 2013 in the region north of 17°N. The sea surface salinity (SSS) along the shelf showed an increasing trend from south to north during both the years (Figure 2b). The SSS in the region north of 17°N showed marginal variation in both years. However, south of 17°N, in 2003 salinities were about 1 psu higher than that of 2013

Surface chlorophyll *a*, based on in-situ measurements, showed an increase from south to north during both 2003 and 2013 (Figure 2c). However, the values in 2003 were much less than that of 2013. For example, in the south, from 8 to 15°N, the values were around 0.1 and 0.2 mg/m<sup>3</sup> in 2003 and 2013 respectively, except at 11°N in 2013 where it was 0.5 mg/m<sup>3</sup>. North of 15°N, the chlorophyll *a* values in 2013 were 3 times higher than that of 2003, indicating enhanced biological productivity. The highest value of 1.8 mg/m<sup>3</sup> was at 20°N in 2013. A pertinent question is whether the observed elevated levels of chlorophyll *a* in 2013 compared to 2003 is driven by transient processes such as coastal Kelvin wave propagation or coastal upwelling. During winter, when the observation is taken, EAS experiences the propagation of coastally trapped downwelling Kelvin wave with high sea level hugging the coast. An examination of sea level anomaly (SLA) maps (Supplementary Figure 1) showed that the SLA all along the coast during 2013 was much higher compared to 2003. A downwelling Kelvin wave will depress the thermocline/nutricline, which in turn will result in the reduction in chlorophyll biomass. Note that, in spite of the deeper SLA, the chlorophyll biomass in 2013 was much higher. Hence, we discount this process as a primary factor in modulating the chlorophyll. It will be shown later that the observed enhancement in the chlorophyll during 2013 may be explained in the context of strengthening of coastal current under section 3.2.

Consistent with the SST (Figure 2a), the vertical thermal structure also revealed a similar pattern of variability for both the years (Figure 2 d & g) with warm waters in the region south of 17°N, and cold and vertically well-mixed waters towards the north, except north of 18°N below 60 m in 2003 (Figure 2d). The salient feature of the thermal structure was the presence of inversion in the south during both years, but with varying spatial extent. During 2003 the thermal inversion, with a magnitude of 0.5°C, was located vertically between 40 and 75 m, while latitudinally it was seen between 8 and 10.5°N. In 2013 (Figure 2g), though the strength of the inversion was same as that of 2003, it was vertically expanded towards shallower depths and latitudinally displaced towards the north. The vertical extend was from 20 to 75 m, while the latitudinal extend was from 11 to 14.5°N. In the north the water column was colder by 0.5°C in 2013 in comparison with 2003 and the vertically well-mixed isothermal layer extended right up to the bottom in 2013.

The vertical salinity structure, on the other hand, showed low salinity waters in the south and high salinity waters towards north (Figure 2 e & h). Vertical salinity distribution during 2003 showed a strong salinity front in the upper 50 m south of 14.5°N (Figure 2e). Within the front salinity increased by 1.4 psu towards north from 34.0 psu. This was the signature of intrusion of low salinity waters of BoB origin. A prominent subsurface high salinity core, with a value of 36 psu, was situated below 40 m between 12.5 and 19.5°N, which shoaled up to 30 m towards the north. This is the Arabian Sea high salinity water mass (ASHSW), which forms in the northern AS during winter, having a characteristic range of temperature and salinity of 24-28°C and 35.3-36.7 psu respectively [Prasanna Kumar and Prasad, 1999]. This water mass occurs in the upper 100 m of the water column between 22.8 and 24.5 sigma-t levels. Another salinity front, with weak gradient was noticed north of 20°N, with the salinity increasing from 36 psu to 36.4 psu. The vertically homogeneous salinity and temperature in the north indicated the formation of ASHSW. Note that the 36 psu isohaline contour in the north was detached from the subsurface closed isohaline contour located in the south in 2003. Though the general pattern of distribution in 2013 (Figure 2h) was similar to that of 2003, there were distinct differences. For example, the low salinity waters seen in the surface layer in the south was 0.6 psu fresher in 2013 as compared to 2003. In addition, the water with 34 psu salinity which was situated in the upper 30m in 2003 was seen deepening to 50 m during 2013. Concomitant with this, the low salinity water also showed an extension from 9°N to 13°N, indicating further northward intrusion of low salinity waters. Another difference was the lack of the salinity front in the north, which was replaced by a homogeneous water column with 36 psu salinity from 19

to 21°N. The extension of the 36 psu salinity contour from surface at 19°N to subsurface up to 13°N indicated the southward spreading of ASHSW formed in the north.

The vertical distribution of chlorophyll *a* in both the years (Figure 2 f & i) essentially reflected a pattern similar to that of the latitudinal variation of surface chlorophyll *a*. The salient feature of the vertical distribution was the presence of high chlorophyll *a* in the upper 60m of the water column in the north. In 2003 the region of high chlorophyll *a* was located north of 20°N, while in the south the water column had very low chlorophyll *a* (Figure 2f). However, south of 15°N, the chlorophyll *a* showed a weak enhancement between 40 and 60m indicating the presence of weak subsurface chlorophyll maximum (SCM). Note that SCM is characteristic feature of the vertical distribution of chlorophyll when upper ocean waters are oligotrophic. This is the case in the southern part of EAS, except during June to September when southwest monsoon upwelling drives phytoplankton blooms. In 2013 the region of high chlorophyll *a* showed a latitudinal expansion, occurring from north of 16°N (Figure 2i). Note the enhancement of the surface chlorophyll *a* at 11°N in 2013, which joins with the SCM located between 40 to 70m. This surface chlorophyll enhancement during 2013 is linked to the strengthened intrusion of BoB waters into the southern part of the EAS, as will be shown in the next section 3.2. It has been shown earlier that the advection of BoB waters during winter brings along with it nutrients, which results in the enhancement of surface chlorophyll in the southern part of the EAS [Prasanna Kumar *et al.*, 2004].

Thus, based on the analysis of the in-situ data during both the years, we infer the (1) occurrence of thermal inversion and (2) intrusion of the low salinity waters of the BoB origin, both in the southern part of the EAS, (3) winter cooling and formation of the ASHSW in the northern part of the EAS and its advection towards south, and (4) northward enhancement of chlorophyll *a*. These are the characteristics features of the regional oceanography of the EAS during winter. It is amply evident from the above analysis of the in-situ data along the EAS that the winters of 2002 (2003 data) was distinctly different from that of 2012 (2013 data) in two aspects: (1) the magnitude and spatial extension of the intrusion of low salinity waters at the southern parts of the EAS and (2) the intensity of winter cooling in the northern part of the EAS and associated response in terms of chlorophyll *a* biomass. We seek explanations for the above two aspects that showed differences between two winters in the following sections.

### **3.2 Link with long-term variability**

In order to understand whether the observed changes are a part of the long-term variability in the regional oceanography prevailing in the EAS during winter, we examined the long-term ICOADS

SST from 1960 to 2015 in the study domain, which is divided into northern and southern boxes (Figure 1). The box-averaged 60-month running mean monthly SST in both the boxes showed a dominant decadal cycle until mid-nineties, and a disruption in the decadal cycle thereafter, with an overall linear warming trend (Figure 3a), a result similar to that obtained by *Prasanna Kumar et al.* [2009] for the basin-averaged SST in the AS. However, during the decade, 2003 to 2013, the SST in the southern box showed an increasing trend ( $0.08^{\circ}\text{C}$ ), while that in the northern box showed a declining trend ( $0.13^{\circ}\text{C}$ ). A similar pattern of variability was also seen when only winter-time (DJF) SST was considered (Figure 3b). The cooling trend observed in the northern EAS during the decade under study would need an explanation. It will be shown subsequently that this decline of SST and the cooling trend in the northern part of the EAS was linked to long-term increase in the strength of the wind.

Unlike the SST, long-term surface salinity data are not available in EAS and hence we used Argo salinity data available from 2001 onwards. The Hovmuller diagram (Figure 4a) showed the presence of low salinity waters, with salinity less than 33.7 psu, confined to the southern latitudes between 8 and 10 and salinity in excess of 36 psu north of  $18^{\circ}\text{N}$  in the EAS. Three episodes of excess freshening was noticed, the 1<sup>st</sup> during 2001-2003, 2<sup>nd</sup> during 2004-2006 and the 3<sup>rd</sup> during 2010-2014, the last episode being more intense with a drop of 0.4 psu compared to the first and second events. During these 3 freshening events, the waters with salinity less than 33.7 psu was seen extending to latitudes up to  $13^{\circ}\text{N}$ . Recall that this excess freshening had its subsurface foot print by way of deepening and spreading of low salinity waters (Figure 2h). The obvious question is what caused the episodic enhancement in the freshening of surface salinity. As southern part of the EAS experiences winter-time freshening due to advection of low salinity waters of the Bay of Bengal origin [*Prasanna Kumar et al.*, 2004], we examined the time-variation of WICC (Figure 4b) and EICC (Figure 4c) in January by analyzing the  $v$ -component of the geostrophic currents for the period 2000 to 2016. Three periods of increased velocity, negative along the southern parts of the east coast of India (EICC, Figure 4c) and positive along the west coast of India (WICC, Figure 4b), were discernible, that approximately coincided with the periods of enhanced freshening. For example, the southward EICC showed a strengthening during all the 3 periods of freshening (Figure 4c). Commensurate with this a strengthening of northward WICC was also evident (Figure 4b). Note that the extended duration of freshening of the 3<sup>rd</sup> episode was associated with the extended duration of strengthening of both EICC and WICC. Though the timing of intensification of EICC/WICC was closely linked to the increased freshening events, the location of the enhancement of EICC/WICC during the 1<sup>st</sup> event was different from the rest. During 2<sup>nd</sup> and 3<sup>rd</sup> freshening events, the

intensification of EICC/WICC was spatially seen from 8°N to 15°/13°N. However, during the 1<sup>st</sup> freshening event the EICC/WICC intensification was noticed from 11°/10°N to 15°/13°N. Hence, we propose that the observed excess freshening episodes in the southern part of the EAS were linked to the increased transportation of low salinity waters of the BoB origin, by a combination of strengthened EICC and WICC. In addition to this, the anomalous freshening episodes in the BoB associated with enhanced precipitation events reported by *Pant et al.* [2015] during July-September of 2006, 2011 and 2012 also would have its contribution to the observed freshening episodes along the southern part of the EAS. It is pertinent to state here that an increase in the precipitation would also contribute to increased fresh water discharge from the Ganges-Brahmaputra river system into the Bay of Bengal reducing the surface water salinity (for example, *Papa et al.*, 2012; *Chaitanya et al.*, 2015).

### **3.3 Implication for chlorophyll *a* biomass**

It is thus clear that the differential spatio-temporal response captured in the in-situ measurements over a period of decade is not an isolated event, but forms a part of the long-term variability experienced by the EAS as well as episodic remote forcing from the BoB. To understand the implication, winter-time (DJF) satellite derived chlorophyll *a* pigment concentrations from MODIS were examined in the southern (Figure 4d) and northern (Figure 4e) boxes from 2002 to 2014. In the southern box, the chlorophyll *a* showed a declining trend with a slope of 0.10 mg/m<sup>3</sup>, while that in the northern box showed an increasing trend with a slope of 0.14 mg/m<sup>3</sup> for the period from 2002 to 2014. This is consistent with the trends in the north-south SST pattern in the EAS and could be understood in the context of prevailing regional oceanography of this region during winter. In the south EAS the increased warming trend in SST coupled with increased episodic freshening leads to an increase in the stratification of the water column, which is evident from the vertical profile of the static stability parameter during 2003 and 2013 (Supplementary Table 1). The value of the static stability parameter is higher by one order-of-magnitude between 2013 and 2003, especially in the upper 25m water column; up to 45m the values are still twice higher in 2013. This depicts the increase in strength of the static stability of the water column during 2013. This increased stratification in turn leads to a decrease in the amount of nutrients that could be made available to the upper ocean through wind-mixing, resulting in the observed decline in chlorophyll *a* biomass. The increased chlorophyll *a* between 2003 and 2013, based on in-situ measurements, could be explained in the context of strengthening of the WICC. The increase in the strength of WICC in 2013 in comparison to 2003 could potentially transport more chlorophyll as well as nutrient rich waters from



the Indo-Sri Lanka region towards the southern part of EAS [Prasanna Kumar et al. 2004] leading to the observed higher levels of chlorophyll.

In the northern EAS the decreasing SST indicated the enhanced winter cooling. To understand what caused the cooling, we examined the winter-time (DJF) wind speed from 1960 to 2015 in the southern (Figure 4f) and northern (Figure 4g) boxes. In both the boxes the wind speeds showed a long-term (0.03 m/s per year for the period 1960-2014) as well as decadal (0.05 m/s per year for the northern box and 0.12 m/s per year for the southern box during the period 2002-2014) increase. The observed chlorophyll *a* enhancement only in the northern box, in spite of the increase in wind speed in both the boxes, could be explained as follows. In the north the increased wind speed during the study period leads to enhanced evaporative cooling of the surface waters as inferred from the 3°C lower SST in 2013 in comparison to 2003. This led to an increase in the convective mixing in the upper water column resulting in the injection of more nutrients to surface waters thereby increasing the chlorophyll *a* biomass as observed. Though direct wind-mixing could be a process that could potentially increase the mixing and deepen the mixed layer in the north, in terms of its magnitude the mixed layer deepening under winter convection by far overwhelms the former [Madhupratap et al., 1996; Prasanna Kumar and Prasad, 1996]. In the south, however, the increase in the wind speed did not result in enhancing the chlorophyll as the increased stratification prevented deep wind-mixing.

#### **4. Summary and concluding remarks**

Using two sets of ship-based in-situ water column data collected during 2<sup>nd</sup> week of January to 1<sup>st</sup> week of February in 2003 and 2013 from the same stations along the EAS using same protocol and a host of remote sensing data, the variability of this region over the decade was examined. The changes inferred from the vertical distributions of thermo-haline and chlorophyll *a* structure of the water column revealed distinct and differential response of EAS, a region of complex interplay between spatially and temporally varying oceanographic processes, to both local and remote forcing. The warming of the southern part of the EAS over the decade was in tandem with the long-term warming experienced by the AS. However, the three episodes of freshening experienced by the southern part of the EAS was not locally forced, but remotely controlled by the strengthening of the winter-time southward EICC and northwards WICC which transported the low salinity BoB waters into the AS. The northern part of the EAS experienced a long-term warming and showed a cooling trend over the decade in which measurements were undertaken. This cooling trend was in response to the strengthening winds in the EAS regions, which resulted in deep convective-mixing. This in turn was potentially capable of supplying increased amount of nutrients to the upper water column, which

enhanced phytoplankton growth and build up of chlorophyll biomass. In contrast, the increasing wind speed in the southern part of the EAS was not strong enough to break the thermo-haline stratification to initiate deep wind-mixing. This curtailed the vertical supply of subsurface nutrients to the upper waters to fuel the growth of phytoplankton and build up of chlorophyll biomass.

Our results points to the fact that though the AS is subjected to similar basin-wide seasonal forcing brought about by the semi-annually reversing monsoons, the water column response in different parts of the basin could be quite different. The limitation of the present study is the lack of co-located nutrient measurements that would have more readily revealed the coupling between the water column changes and ecosystem response via alterations in nutrient concentrations. What is needed is a co-located long time-series measurements of physical and biogeochemical properties to address the inter-annual to multi-decadal time scale variability which is least known in this part of the world ocean. This calls for the development of either a mooring with physical and biogeochemical sensors or ship-based repeat transects on a sustained basis, augmented by an equally strong modelling efforts.

### **Acknowledgement**

The authors thank Director CSIR-National Institute of Oceanography (CSIR-NIO), Dona Paula, Goa and Council of Scientific and Industrial Research (CSIR), New Delhi for all the support and encouragement for this research. The authors thank Dr. Subha Sathyendrnath and anonymous reviewers for the constructive criticism which helped to improve the manuscript. The authors also thank the participants of FORV *Sagar Sampada* and RV *Sindhu Sadhana*, specially Ms. Reshma, Mr. Navneeth, Ms. Valetta, Ms. Sulekha, Ms. Manisha Coelho, Mr. Kirthan and Mr. Shyam for helping with the diagrams. This work forms a part of 3 projects (1) “Mineral dust fluxes and impact on ocean and coastal ecosystem” under GEOSINK, (2) “Impact of climate change and rapid warming of the Arabian Sea on Indian Monsoon and bioresources (IC-RASI)” both funded by CSIR, and (3) "Environmental studies for Myctophid resources assessment in the Arabian Sea" funded by MoES through CMLRE, Kochi . We thank NASA ocean biology group for providing MODIS Aqua ocean color data, ICOADS for wind and SST data, JAMSTEC for gridded ARGO data, AVISO for altimeter data (see section 2 for details). In-situ cruise data can be provided by the Data Centre of the CSIR-National Institute of Oceanography, Goa, India ([www.nio.org](http://www.nio.org)). This is NIO contribution number XXXX.

## Figure Captions

**Figure 1** Schematics depicting regional oceanographic processes operating within the eastern Arabian Sea (EAS). During winter monsoon low salinity Bay of Bengal (BoB) water is transported into the southern part of the EAS, while the northern part of EAS comes under the influence of winter convection and formation of Arabian Sea high salinity water mass which advects southward. A down-welling Kelvin wave propagates along the western boundary of the BoB as well as coastal boundary of the EAS which drives the southward flowing East India Coastal Current (EICC) along east coast of India and northward flowing west India coastal current (WICC) along west coast of India during winter. This Kelvin wave also drives a westward propagating down-welling Rossby waves from the coastal boundary of EAS. A mini warm pool develops in the southern part of the EAS during spring-summer period (March-May). See text for details. The filled circles in blue indicate the station locations for in-situ measurements during 2003 and 2013, while those in red are the location for the computation of v-component of geostrophic velocity. The shaded boxes in north and southern EAS represent the region over which ICOADS SST, wind and MODIS aqua chlorophyll *a* data were averaged.

**Figure 2** Latitudinal variation of surface (a-c) and vertical (d-i) distributions of temperature ( $^{\circ}\text{C}$ ) (a,d,g), salinity (psu) (b,e,h) and chlorophyll *a* ( $\text{mg}/\text{m}^3$ ) (c,f,i) for 2003 (d,e,f) and 2013 (g,h,i) based on in-situ measurements. The red and blue colour shading in temperature (d & g) represents warm and cold waters respectively, while in salinity (e & h) magenda and blue colour shading represents high and low salinity waters respectively.

**Figure 3** Box-averaged (a) 60-month running mean of monthly mean SST ( $^{\circ}\text{C}$ ) and (b) 5-year running mean winter-time (DJF) SST ( $^{\circ}\text{C}$ ) from ICOADS data for the period 1960 to 2015. Note that the linear trends in the SST in the northern and southern boxes in (a) were  $0.57^{\circ}\text{C}$  and  $0.49^{\circ}\text{C}$  respectively for 55 years (1960-2015), while that for 10 years (2003-2013) coinciding with study period were  $-0.13^{\circ}\text{C}$  and  $0.08^{\circ}\text{C}$  respectively. Similarly, the liner trends in the SST for winter in the northern and southern boxes in (b) were  $0.58^{\circ}\text{C}$  and  $0.49^{\circ}\text{C}$  respectively for 55 years, while that for 10 years coinciding with study period were  $-0.14^{\circ}\text{C}$  and  $0.07^{\circ}\text{C}$  respectively.

**Figure 4** Hovmuller plot of (a) January time surface salinity at stations along the SEA (see figure 1 for station location) from gridded Argo data for the period 2001 to 2016. Salinity less than 33.7 psu is shaded in white (b) v-component of the geostrophic currents—along west and (c) east coasts of India during all the January from 2001 to 2016 (see figure 1 for station location) derived from AVISO merged product. The positive and negative values indicate the northward and southward currents respectively. The box-averaged monthly mean chlorophyll *a* ( $\text{mg}/\text{m}^3$ ) derived from MODIS aqua for the period 2002 to 2014 is in (d & e), while wind (m/s) derived from ICOADS data for the period 1960 to 2014 is in (f & g). The dashed lines in (d) to (g) are the linear trend lines. See text for details.

## References

- Chaitanya, A.V.S., F. Durand, S. Mathew, V.V. Gopalakrishna, F. Papa, M. Lengaigne, J. Vialard, C. KranthiKumar, and R. Venkatesan (2015), Observed year-to-year sea surface salinity variability in the Bay of Bengal during the 2009–2014 period, *Ocean Dynamic*, 65, 173–186.
- Durand, F., S. R. Shetye, J. Vialard, D. Shankar, S. S. C. Shenoi, C. Ethe, and G. Madec (2004), Impact of temperature inversions on SST evolution in the southeastern Arabian Sea during the pre-summer monsoon season, *Geophys. Res. Lett.*, 31, L01305, doi:10.1029/2003GL018906.

Hareesh Kumar, V. H., M. Joshi, K. V. Sanilkumar, A. D. Rao, P. Anand, K. A. Kumar, and C. V. K. P. Rao (2009), Growth and decay of the Arabian Sea mini warm pool during May 2000: Observations and simulations, *Deep Sea Res-I*, 56, 528–540, doi:10.1016/j.dsr.2008.12.004.

Joseph, P. V. (1990), Warm Pool over the Indian Ocean and Monsoon Onset, *Tropical Ocean-Atmos. News Lett.*, 53, 1–5.

Kurian, J., and P. N. Vinayachandran (2006), Formation mechanisms of temperature inversions in the southeastern Arabian Sea, *Geophys. Res. Lett.*, 33, L17611, doi:10.1029/2006GL027280.

Madhupratap, M., Kumar, S.P, Bhattathiri, P.M.A, Kumar, M.D, Raghukumar, S, Nair, K.K.C, and Ramaiah. N (1996), Mechanisms of the biological response to winter cooling in the northeastern Arabian Sea, *Nature.*, 384, 549–552.

Naqvi, S.W. A., D.A. Jayakumar, P.V. Narvekar, H. Naik, V.V.S.S. Sarma, W, D'Souza, S. Joseph, and M.D.George (2000), In-creased marine production of N<sub>2</sub>O due to intensifying anoxia on the Indian continental shelf, *Nature.*, 408, 346–349, 2000.

Nyadjro, E. S., B. Subrahmanyam, V. S. N. Murty, and J. F. Shriver (2012), The role of salinity on the dynamics of the Arabian Sea mini warm pool, *J. Geophys. Res.*, 117, C09002, doi:10.1029/2012JC007978.

Papa, F., S. K. Bala, R. K. Pandey, F. Durand, V. V. Gopalakrishna, A. Rahman, and W. B. Rossow (2012), Ganga-Brahmaputra river discharge from Jason-2 radar altimetry: An update to the long-term satellite-derived estimates of continental freshwater forcing flux into the Bay of Bengal, *J. Geophys. Res.*, 117, C11021, doi:10.1029/2012JC008158.

Prasanna Kumar, S., and T.G.Prasad (1996), Winter cooling in the northern Arabian Sea, *Current Sci.*, 71, 834–841.

Prasanna Kumar, S., J. Narvekar, A. Kumar, C. Shaji, P. Anand, P. Sabu, G. Rijomon, J. Josia, K.A. Jayaraj, A. Radhika, K.K.C. Nair ( 2004), Intrusion of the Bay of Bengal water into the Arabian Sea during winter monsoon and associated chemical and biological response, *Geophys. Res. Lett.*, 31, L15304, doi:10.1029/2004GL020247.

Prasanna Kumar, S., R.P. Roshin, J. Narvekar, P.K. Dinesh Kumar, E. Vivekanandan (2009), Response of the Arabian Sea to global warming and associated regional climate shift, *Mar Env. Res.*, 68, 217–222.

Prasanna Kumar, S. and T.G. Prasad (1999), Formation and spreading of Arabian Sea high saline water mass, *J. Geophys. Res.*, 104, 1455-1464.

Dinesh Kumar.P.K, ,Y. Steeven Paul, K.R. Muraleedharan, V.S.N. Murty and P.N. Preenu (2016), Comparison of Long-term variability of Sea Surface Temperature in the Arabian Sea and Bay of Bengal, *Reg. Stud. Mar. Sci.*, vol.3; 2016; 67-75.

Pond, S., and G.L. Pickard (1983), *Introductory Dynamical Oceanography*. 2nd edition, 329pp, Butterworth-Heinemann.

- Pant, V., M. S. Girishkumar, T. V. S. Udaya Bhaskar, M. Ravichandran, F. Papa, and V. P. Thangaprakash (2015), Observed interannual variability of near-surface salinity in the Bay of Bengal. *J. Geophys. Res. Oceans*, 120, 3315–3329, doi:10.1002/2014JC010340.
- Rao, R. R., and R. Sivakumar (1999), On the possible mechanisms of the evolution of a mini-warm pool during the pre-summer monsoon season and the genesis of onset vortex in the southeastern Arabian Sea, *Q. J. R. Meteorol. Soc.*, 125, 787–809.
- Roxy, M. K., K. Ritika, P. Terray, and S. Masson (2014), The curious case of Indian Ocean warming, *J. Clim.*, 27, 8501–8509
- Sanilkumar K.V., P. V Hareesh Kumar, Jossia K Joseph, and J.K. Panigrahi (2004), Arabian Sea mini warm pool during May 2000, *Curr. Sci.*, 86, 10–105.
- Smitha, B. R., V. N. Sanjeevan, K. G. Vimalkumar, and C. Revichandran (2008), On the Upwelling off the Southern Tip and along the West Coast of India, *J. of Coastal Res.*, 24, 95–102.
- Shetye, S.R., Gouveia, A.D, Shenoi, S.S.C, Michael, G.S, Sundar, D, Almedia, A.M, and Santanam. K (1991), The coastal current off western India during the northeast monsoon, *Deep-Sea Res.*, 38, 1517-1529.
- Thadathil, P., and A. Gosh (1992), Surface layer temperature inversion in the Arabian Sea during winter, *J. Oceanogr.*, 48, 293–304.
- UNESCO. (1994), Protocols for the joint global ocean flux study (JGOFS), *Manual and Guides* 29, pp. 170.
- Vinayachandran, P. N., D. Shankar, J. Kurian, F. Durand, and S. S. C. Shenoi (2007), Arabian Sea mini warm pool and the monsoon onset vortex. *Curr. Sci.*, 93(2), 203-214.
- Wyrtki, K. (1971), *Oceanographic Atlas of the International Indian Ocean Expedition*, 531 pp., U.S. Gov. Print. Off., Washington, D. C.
- Woodruff, S.D., S.J. Worley, S.J. Lubker, Z. Ji, J.E. Freeman, D.I. Berry, P. Brohan, E.C. Kent, R.W. Reynolds, S.R. Smith, and C. Wilkinson (2011), ICOADS Release 2.5: Extensions and enhancements to the surface marine meteorological archive. *Int. J. Climatol.*, 31, 951-967, doi:10.1002/joc.2103

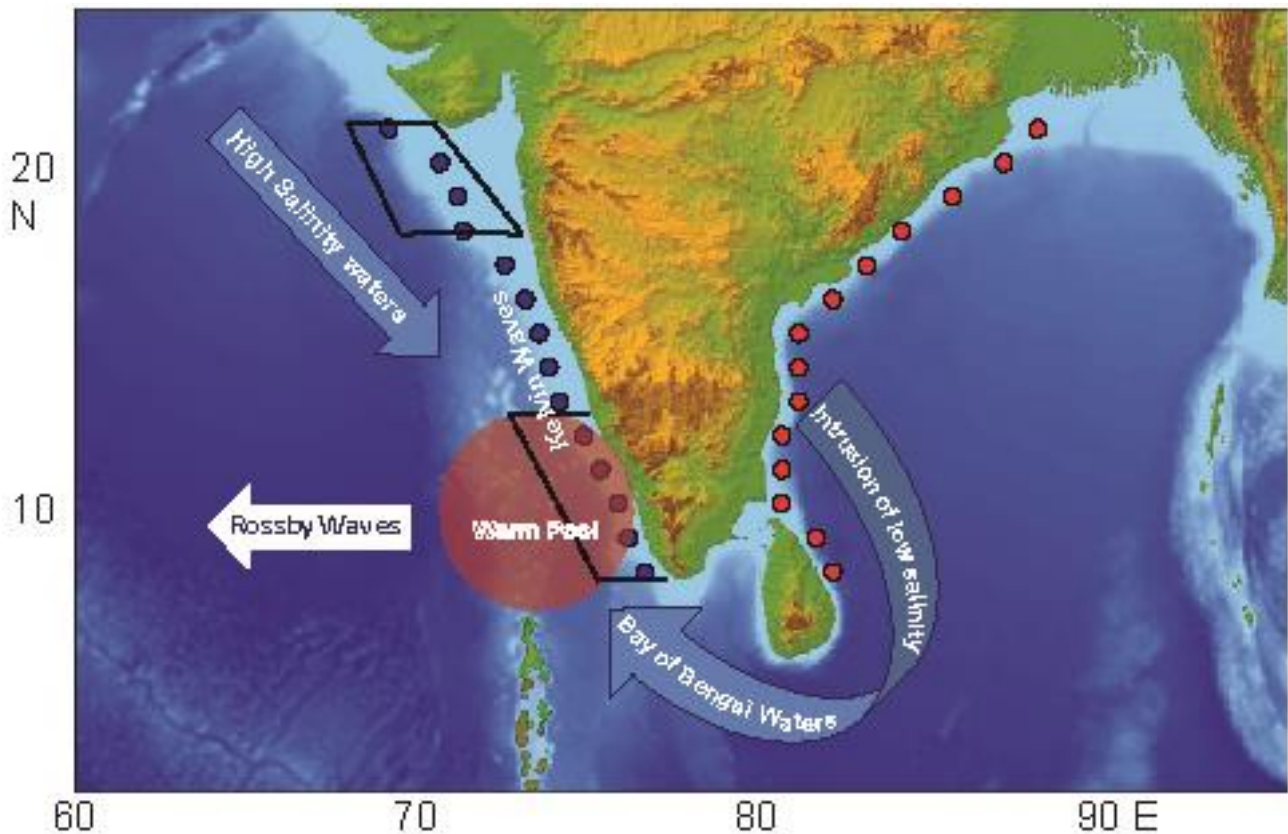


**Figure 1** Schematics depicting regional oceanographic processes operating within the eastern Arabian Sea (EAS). During winter monsoon low salinity Bay of Bengal (BoB) water is transported into the southern part of the EAS, while the northern part of EAS comes under the influence of winter convection and formation of Arabian Sea high salinity water mass which advects southward. A down-welling Kelvin wave propagates along the western boundary of the BoB as well as coastal boundary of the EAS which drives the southward flowing East India Coastal Current (EICC) along east coast of India and northward flowing west India coastal current (WICC) along west coast of India during winter. This Kelvin wave also drives a westward propagating down-welling Rossby waves from the coastal boundary of EAS. A mini warm pool develops in the southern part of the EAS during spring-summer period (March-May). See text for details. The filled circles in blue indicate the station locations for in-situ measurements during 2003 and 2013, while those in red are the location for the computation of v-component of geostrophic velocity. The shaded boxes in north and southern EAS represent the region over which ICOADS SST, wind and MODIS aqua chlorophyll *a* data were averaged.

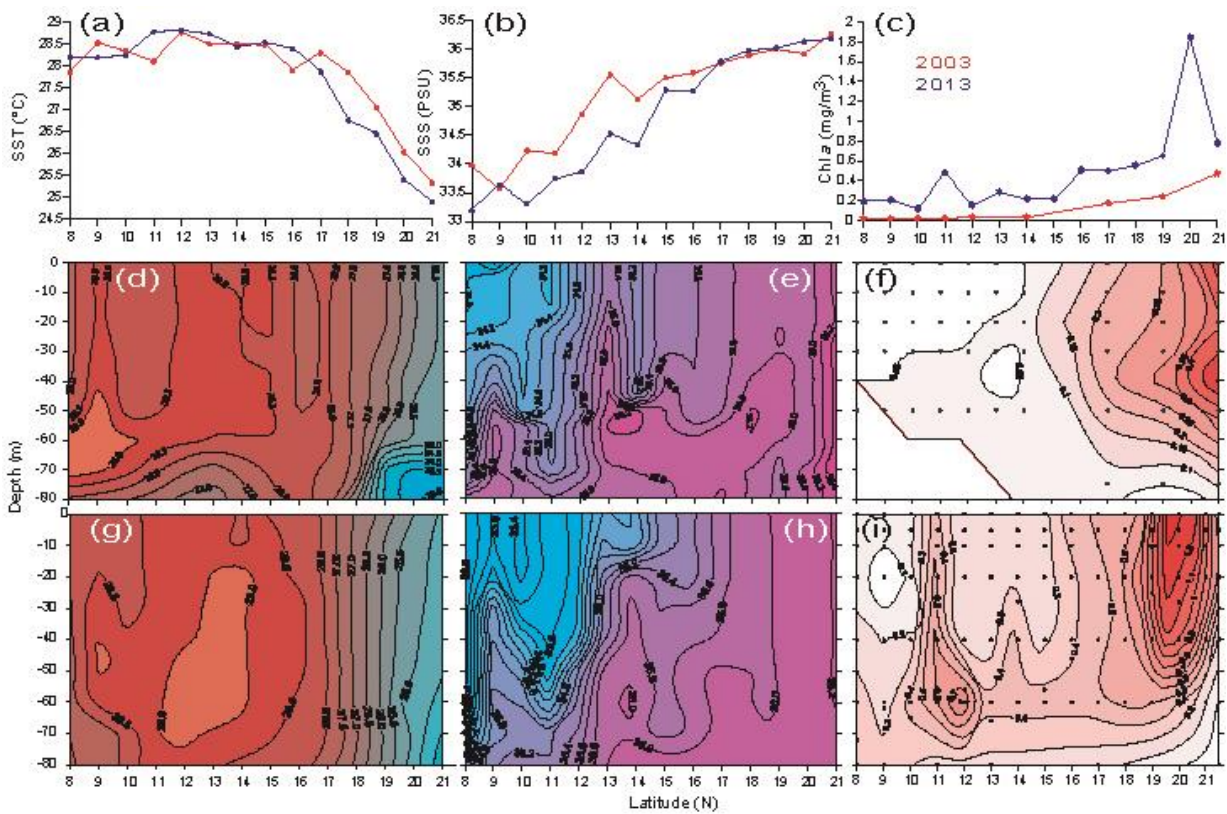


**Figure 2** Latitudinal variation of surface (a-c) and vertical (d-i) distributions of temperature ( $^{\circ}\text{C}$ ) (a,d,g), salinity (psu) (b,e,h) and chlorophyll *a* ( $\text{mg}/\text{m}^3$ ) (c,f,i) for 2003 (d,e,f) and 2013 (g,h,i) based on in-situ measurements. The red and blue colour shading in temperature (d & g) represents warm and cold waters respectively, while in salinity (e & h) magenta and blue colour shading represents high and low salinity waters respectively.

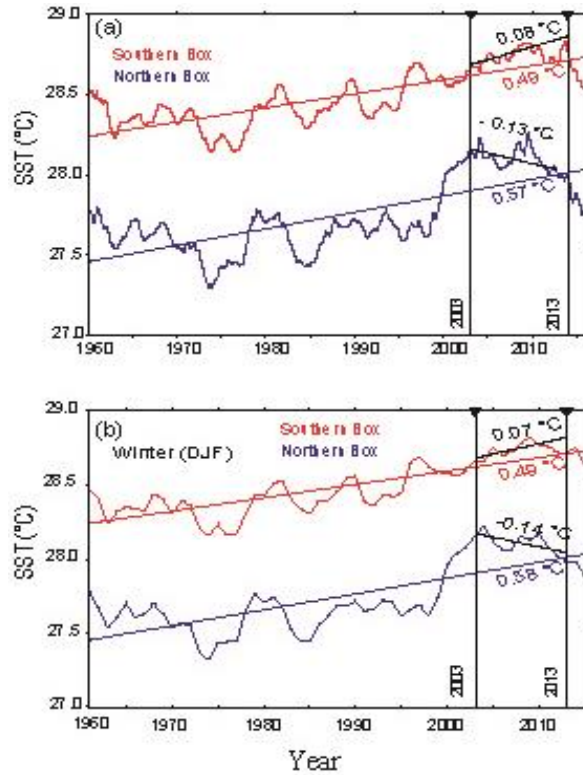


**Figure 3** Box-averaged (a) 60-month running mean of monthly mean SST (°C) and (b) 5-year running mean winter-time (DJF) SST (°C) from ICOADS data for the period 1960 to 2015. Note that the linear trends in the SST in the northern and southern boxes in (a) were 0.57°C and 0.49°C respectively for 55 years (1960-2015), while that for 10 years (2003-2013) coinciding with study period were -0.13°C and 0.08°C respectively. Similarly, the linear trends in the SST for winter in the northern and southern boxes in (b) were 0.58°C and 0.49°C respectively for 55 years, while that for 10 years coinciding with study period were -0.14°C and 0.07°C respectively.



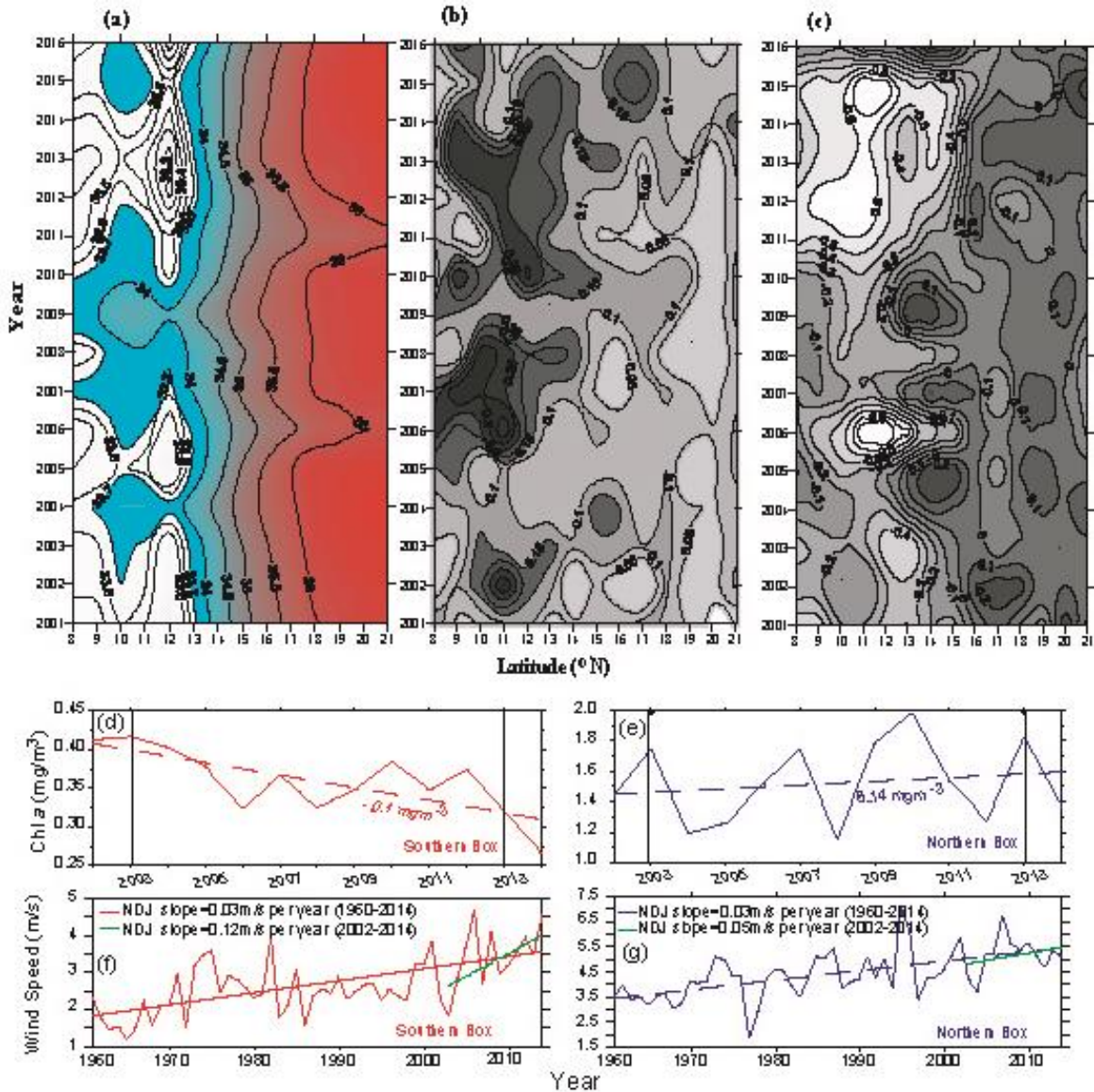


**Figure 4** Hovmuller plot of (a) January time surface salinity at stations along the SEA (see figure 1 for station location) from gridded Argo data for the period 2001 to 2016. Salinity less than 33.7 psu is shaded in white (b) v-component of the geostrophic currents—along west and (c) east coasts of India during all the January from 2001 to 2016 (see figure 1 for station location) derived from AVISO merged product. The positive and negative values indicate the northward and southward currents respectively. The box-averaged monthly mean chlorophyll *a* ( $\text{mg}/\text{m}^3$ ) derived from MODIS aqua for the period 2002 to 2014 is in (d & e), while wind ( $\text{m}/\text{s}$ ) derived from ICOADS data for the period 1960 to 2014 is in (f & g). The dashed lines in (d) to (g) are the linear trend lines. See text for details.

## Supporting Information for

[Winter-time variability of the Eastern Arabian Sea – A comparison between 2003 and 2013]

[Jayu Narvekar, Joshua Rosario D’Mello, S. Prasanna Kumar\*, Priyanka Banerjee<sup>1</sup>, Vrinda Sharma and Prachi Shenai-Tirodkar]

[CSIR-National Institute of Oceanography, Dona Paula, Goa-403 004, India.

<sup>1</sup>Centre for Atmospheric and Oceanic Sciences, Indian Institute of Science, Bangalore, India]

\* Corresponding author

### Contents of this file

Tables S1

Depth (m)	Static stability parameter (Ex $10^{-5}$ , $m^{-1}$ )	
	2003	2013
5	0.0089	0.4167
15	0.0686	0.7783
25	0.0215	0.7651
35	0.3226	0.7794
45	0.4032	0.8271

### Additional Supporting Information (Files uploaded separately)

Captions for Tables S1

The static stability parameter ( $E$ ,  $m^{-1}$ ) with depth at 8°N station located within the southern box in the EAS during 2003 and 2013

## Supporting Information for

[Winter-time variability of the Eastern Arabian Sea – A comparison between 2003 and 2013 ]

[Jayu Narvekar, Joshua Rosario D’Mello, S. Prasanna Kumar\*, Priyanka Banerjee<sup>1</sup>, Vrinda Sharma and Prachi Shenai-Tirodkar]

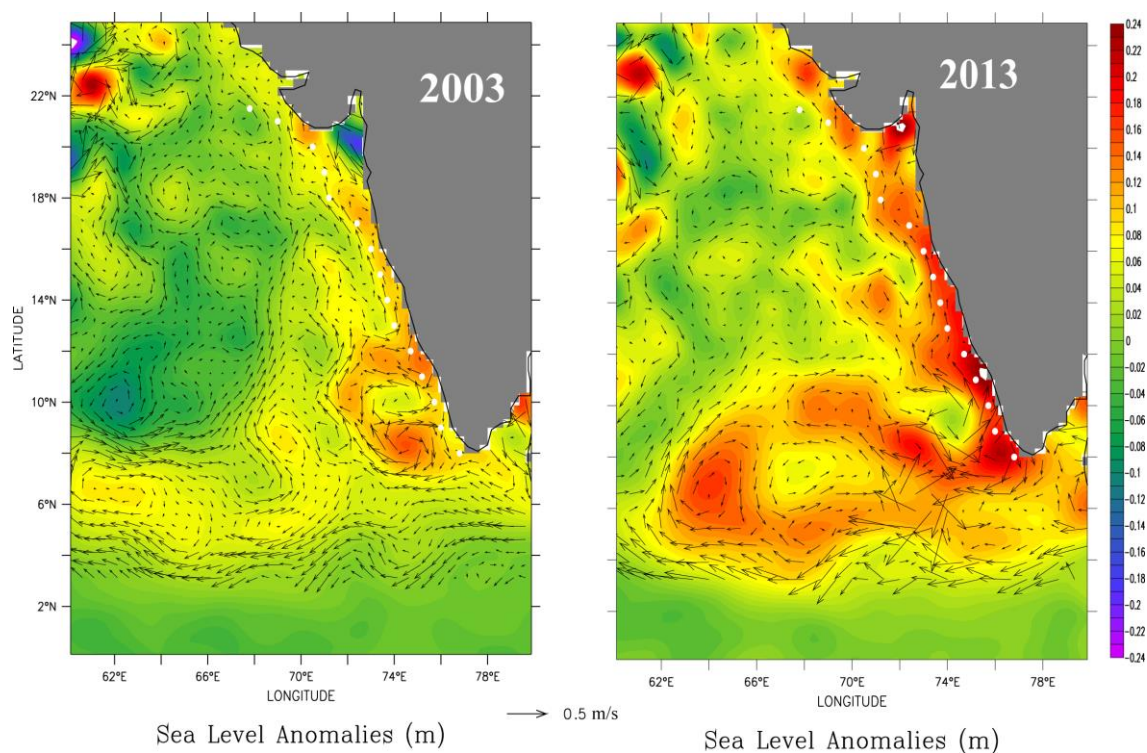
[CSIR-National Institute of Oceanography, Dona Paula, Goa-403 004, India.

<sup>1</sup>Centre for Atmospheric and Oceanic Sciences, Indian Institute of Science, Bangalore, India]

\* Corresponding author

### Contents of this file

Figure S1



### Additional Supporting Information (Files uploaded separately)

#### Captions for Figure S1

Sea Level anomaly overlaid with geostrophic current during January 2003 (left) and January 2013 (right) in the eastern Arabian Sea. White filled circles indicate the station location.